Journal of Statistical Physics, Vol. 107, Nos. 1/2, April 2002 (© 2002)

A Multi-Speed Compressible Lattice-Boltzmann Model

R. J. Mason[1]

Received February 14, 2001; accepted November 9, 2001

An extension of the lattice Boltzmann BGK method to compressible flows is presented that combines three novel additions: (1) particles move density and energy weights in multiple velocity bins (11 for 1-D flow) to nearby cell centers. (2) the equilibrium distribution remains an unexpanded Maxwellian; and (3) transport and relaxation to equilibrium are performed implicitly at each node. These advances allow for the parallel modeling of high Mach number shocks and high Reynolds number flows, while avoiding advective numerical diffusion, the need for Riemann solvers, and non-linear limiters. A 1D shock tube application is shown. Generalization to higher dimensions and multi-materials are discussed.

KEY WORDS: Compressible hydrodynamics; Euler equations; Lattice gas; BGK equation; particle-in-cell.

1. INTRODUCTION

The Lattice Boltzmann method (LBM) provides efficient parallel simulation of low speed Eulerian hydrodynamic flows. It employs an underlying kinetic model based on a distribution of density weights at a set of discrete velocities to obtain solutions to the Euler and Navier–Stokes equations. Lattice gas automata[1] (LGA) were first used for this kinetics, then the Boltzmann equation,[2] and now, generally, a Krook[3] (BGK) collision operator is used to establish equilibrium.[4] LBM has been applied[5] to complex geometries, fluid turbulence, multi-component flows and heat transfer, and multi-dimensions.[6] Here, we introduce a new particle-based compressible lattice-BGK model (CLBM).[7]

Traditional finite-volume compressible Eulerian schemes have seen significant refinement in recent years.[8] These schemes frequently employ

[1] Los Alamos National Laboratory, Applied Physics Division, Los Alamos, New Mexico 87545; e-mail: mason@lanl.gov

0022-4715/02/0400-0385/0 © 2002 Plenum Publishing Corporation

Godunov Riemann solvers,[9] plus advection with total variation diminishing (TVD) and essentially non-oscillatory (ENO) methods[10] to minimize numerical diffusion. They can bear a burden, however, of complex Riemann logic, parallelization and multi-dimensional challenges, residual numerical oscillations, and an uncertain diffusive content. CLBM can offer a robust, embarrassingly parallel alternative and new insight.

The standard LBM[6] model transports a distribution of density weights during a computational time step Δt, typically with one speed for each direction (9 speeds including zero for a 2D simulation). It combines the weights at each speed to form mean fluid densities and velocities. It then constructs a local Maxwellian equilibrium distribution from these mean properties. Finally, LBM relaxes the weights at a rate $1/\tau$ towards this equilibrium. The transport and relaxation operations are split (sequential). The transport operation is linear, and moves the weights to neighboring cell centers over a distance of, say, Δx. The Maxwellian distribution is expanded for small speeds relative to a mesh speed, $\Delta x/\Delta t$. Traditional LBM relaxation is performed explicitly, with τ chosen such that $\tau > \Delta t/2$ for stability.

LBM is largely limited to low speed flows (incompressible), although several related compressible techniques have been propose.[11–20] Alexander *et al.*[11] chose a modified equilibrium distribution, allowing the lattice gas equations replicate the Burgers equation with a controlled sound speed. Nadiga[12] designed a discrete scheme with velocities adapted to the local flow conditions and using limited interpolated fluxes. Huang *et al.*[13] similarly used flow-adapted discrete velocities, a non-unique equilibrium distribution constrained by a set of moments linearly, and interpolated the deposition of weights to the nodes. Prendergast and Xu,[14] Kim *et al.*,[15] and Kotelnikov and Montgomery[16] used the Krook model to evaluate cell boundary fluxes and then employed TVD flux limitation to establish the mean flow into neighboring cells. Renda *et al.*[17] modified the equilibrium distribution at high speeds. Vahala *et al.*[18] extended the Maxwellian expansion, and went to octagonal meshes to achieve Mach numbers of 0.5. Sun[19] used a set of particle velocities adapted to the local fluid velocity and internal energy. De Cicco *et al.*[20] employed additional ring of velocities for shocks, and Guangwu *et al.*[21] supplied both the extra velocities and an added set of energy weights for compressible modeling.

Where these compressible approaches employ flux-limitation and/or interpolation, they introduce uncertain levels of diffusion and clipping that is reminiscent of the traditional finite volume Eulerian schemes, but with added kinetic complexity. Where they add additional velocities and energy weights, but an expanded equilibrium distribution, these methods require the determination of additional moments beyond momentum and energy

for closure, and recourse to ad hoc relations between these moments. We seek to avoid these limitations.

The present CLBM approach resembles comprehensive Rarefied Gas Dynamic schemes,[22] and a much earlier particle-in-cell (PIC) method.[23–25] However, here the number of velocity beams is reduced to a minimum for efficiency in the Eulerian limit, and the particle end points are restricted to cell centers to eliminate numerical diffusion from interpolation and the need for flux-limitation.

In the next section the compressible model is described. Section 3 presents results from a shock tube simulation, along with a phase space rendering of the underlying kinetics. Finally, Section 4 discusses possible extensions, and Section 5 gives concluding remarks.

2. THE COMPRESSIBLE MODEL

The new CLBM is presently based on the 1D Krook equation[4]

$$\frac{\partial f}{\partial t}+u\frac{\partial f}{\partial x}=-v(f-f^{\mathrm{eq}}) \tag{1}$$

in which the equilibrium distribution f^{eq} is given by

$$f^{\mathrm{eq}}(x,u,t)=\frac{n(x,t)}{\sqrt{2\pi}\,a_0(x,t)}\exp\left(-\frac{(u-U(x,t))^2+v^2+w^2}{2a_0^2(x,t)}\right) \tag{2}$$

with n, $\mathbf{u}$, and $a_0^2=\kappa T/m$ the local density, mean velocity and mean thermal speed, respectively, and where κ is Boltzmann's constant, m is the molecular mass, and T is the fluid temperature. In order to transport the transverse temperature data conveniently, we produce two reduced distributions[23, 24, 26] by integrating over the transverse velocities v and w. We thereby obtain a set of density and energy weights $g=\int f\,dv\,dw$, and $h=m\int(v^2+w^2)\,f\,dv\,dw$, governed by

$$\frac{\partial g_j}{\partial t}+u_j\frac{\partial g_j}{\partial x}=\left.\frac{dg_j}{dt}\right|_{\mathrm{col}}=-v(g_j-g_j^{\mathrm{eq}}) \tag{3a}$$

and

$$\frac{\partial h_j}{\partial t}+u_j\frac{\partial h_j}{\partial x}=\left.\frac{dh_j}{dt}\right|_{\mathrm{col}}=-v(h_j-h_j^{\mathrm{eq}}) \tag{3b}$$

at the discrete velocities u, indexed by j. The corresponding reduced equilibria at each velocity are

$$g_j^{\text{eq}} = \frac{n(x,t)}{\sqrt{2\pi}\, a_0(x,t)} \exp\left(-\frac{(u_j - U(x,t))^2}{2a_0^2(x,t)}\right) \tag{4a}$$

and

$$h_j^{\text{eq}} = 2ma_0^2(x,t)\, g_j^{\text{eq}} \tag{4b}$$

The coupling between the weights occurs through the three moments

$$\begin{aligned} n(x,t) &= \sum_j g_j\, \Delta u \\ nU(x,t) &= \sum_j u g_j\, \Delta u \\ 3nma_0^2(x,t) &= 3nkT(x,t) = \sum_j mu_j^2 g_j\, \Delta u + \sum_j mh_j\, \Delta u \end{aligned} \tag{5}$$

which are computed with constant width velocity bins Δu. Our scheme is particle based, so that advection of the weights is accomplished by the motion of particles, here labeled l. The particles are given initial weights according to

$$g_l = \frac{Nn(x_l,t)}{\sqrt{2\pi}\, a_0(x_l,t)} \exp\left(-\frac{(u_l - U(x_l,t))^2}{2a_0^2(x_l,t)}\right) \tag{6a}$$

and

$$h_l = 2ma_0^2(x_l,t)\, g_l \tag{6b}$$

with a normalization N such that the initial particle contributions to each cell add to produce $n(x,t)$. Transport is accomplished by moving weighted particle l from old position $x_l^{(m)}$ to new position $x_l^{(m+1)}$ with speed u_l [equal to one of the beam velocities u_j].

$$x_l^{(m+1)} = x_l^{(m)} + u_l\, \Delta t \tag{7}$$

Weights on the particles are accumulated to evaluate moments in the cells following traditional PIC procedures.[27]

2.1. The Early PIC Approach

In our very earliest one-dimensional studies[23–25] we used 89 velocity beams over the range $\pm 5a_0$. Two or more particles were used per cell in each velocity beam. During a computational cycle the particles were moved relative to a background mesh of fixed cells of width Δx. The time step Δt was chosen so that particles at the mean thermal speed a_0 would cross one cell per cycle, and so that $v\,\Delta t < 1$. Thus, many of the particles crossed less than one cell. Linear area-weighting[27] was employed to attribute the particle density, velocity, and energy to the cell centers (here designated by x_l) and used to determine a cell-centered Maxwellian. This data was interpolated (reverse area-weighted) to produce a local Maxwellian at each particle's position. The particle density and energy weights were changed through explicit relaxation toward this local Maxwellian. Thus, by virtue of the right hand side of Eq. (3a), the transported density weights, $g_l^{(*)}$ [with (*) indicating post-transport, i.e., $g_l^{(m)}(x_l - u_l\,\Delta t)$] would relax through collisions to

$$g_l^{(m+1)} = g_l^{(*)} - v\,\Delta t(g_l^{(+)} - g_l^{\mathrm{eq}(*)}) = (1 - v\,\Delta t)\,g_l^{(*)} + v\,\Delta t\,g_l^{\mathrm{eq}(*)} \tag{8}$$

in which $g_l^{\mathrm{eq}(*)}$, the local Maxwellian, was area weighted to the particle, and based on moments of the transported weights evaluated at the centers. The superscript (+) indicated a possible time level choice, e.g., fully explicit or fully implicit. For explicit collisions $g_l^{(+)}$ was the same as $g_l^{(*)}$ following the transport. The transported energy weights $h_l^{(*)}$ were similarly relaxed. The new particle weights were then area weighted to the nodes to yield the new moments. This early weighted PIC scheme yielded weak shock solutions in agreement with alternate numerical results,[28] but generally broad shock structures. The wide range of particle velocities promised an accurate modeling for Rarefied Gas Dynamics[22] problems, where the particle weight changes from collisions would be minimal. This primary scheme[23–25] was, in fact, an early version of discrete-velocity models (DVM)[29, 30] of the Boltzmann equation, now widely applied in kinetic calculations.

Note that the reduced distribution h_l was used here for one-dimensional flow to transport the *transverse thermal energy* (perpendicular to the fluid drift direction) with improved resolution. Without this reduction many additional speeds would be needed to represent the transverse kinetics. This simplification was first used by Chu[26] for BGK shock studies. An extension of the method to two-dimensional flows (in directions x and y, with corresponding drifts u and v) uses only $h = m \int w^2 f\,dv\,dw$, and employs many additional speeds, as shown by Yang and Huang.[22] A 3D extension would

solve Eq. (1) for the weights f in each cell, using no reduction. In all these cases, total energy in the flow direction is transported by the velocity distribution of the weights. This is in contrast to the internal energy distribution function $g = ((u-\mathbf{U})^2+v^2+w^2)\,f$, introduced by He *et al.*[31] for the transport of thermal energy in the incompressible limit.

2.2. The New CLBM Model

Our new scheme shares many features of our earlier PIC–DVM approach, but now *focuses on the Eulerian limit*. We now seek to use only the smallest number of velocities beams needed to preserve the fluid moments of density, momentum and energy. Learning from traditional LBM,[5] we time-tie our discrete velocity set to our space discretization, producing a discretized version of DVM.[30] However, we differ from earlier approaches in three important respects:

(a) The Velocity Lattice. We now employ much smaller number of beams (11 in one dimension over a range $\pm 5a_0$ for the shocked flow of Section 3) than for kinetic DVM. Also we employ many more beams than would be used in 1D projection for traditional LBM. More importantly, the particle velocities are now in a "lattice," such that all of them move strictly between cell centers on the background mesh, many *skipping* over neighboring cells. The zero-speed particle is, of course, fixed. During a time step the first moving particles (at $\pm a_0$) shift to the nearest neighbors, the next in speed skips one cell, etc., until finally the fastest particles project left or right to the 5th cell center. This arrangement is sketched in Fig. 1. It has the negative consequence that the resultant stencil is large; we must expect that $\geqslant 11$ cells will be needed to resolve a shock. It has the important advantage that interpolative diffusion is eliminated. In Fig. 1 we introduce the concept of a macro-cell as including all the cells reached at the different speeds from a cell center during a cycle.

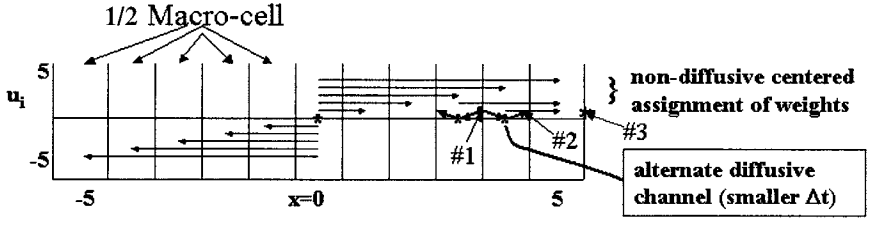

Fig. 1. Velocities are selected to run particles between cell centers in a time step. Eleven cells constitute a Macro-cell. Non cell-centered Particle #1's weights could diffuse to #2 and #3.

Interpolative diffusion could evolve in our earlier model[23] as follows: Assume that a highly weighted particle (#1) has moved right to a cell boundary, and that the initial fluid density is low beyond this boundary. Let the time step Δt be such that the particle moves only a fraction of the cell width Δx. The particle projects its density weight evenly between the two neighboring cells, left and right. This contributes to the Maxwellian amplitude at the right cell center, as shown in Fig. 1. Now consider a similar particle (#2) further right near the next cell boundary. The interpolated local Maxwellian at that particle's location now includes a contribution from particle #1. In the collisional relaxation process particle #2 will have its weights adjusted toward this Maxwellian. In the next cycle particle #2 will project a fraction this new weight into the next cell center to the right, increasing the density of that cell's Maxwellian. This, in turn, will interpolate a fraction its weight to the local Maxwellian for #3, where collisions will subsequently adjust its weights, and so on. Thus, density could diffuse ahead, one cell per time step, an error now avoided with particles stopping only at centers.

(b) An Unexpanded Maxwellian. We continue to leave the Maxwellian unexpanded, thereby permitting modeling at high Mach numbers. (As a byproduct, a more accurate rendering of incompressible LBM should possible for low speed flow in a high background temperature.) Note that for higher speeds flows, and stronger shocks than the one analyzed in Section 3, a greater number and range of velocity beams may be needed to represent the underlying kinetics. In general, the moments over our small number of beams will not be precisely equal[29, 30] to the moments over a full Maxwellian, although for the sample calculations which follow, effects from this are minimal. For the moment sums in Eq. (5) we have used $\Delta u = a_0$. For more precision one might choose more beams and a smaller Δu, or simply renormalize the beams with shifted weights for greater accuracy in the moments.

(c) Implicit collisions. We relax to the Maxwellian implicitly, permitting large collision rates $\nu\,\Delta t \gg 1$ with stability, and possibly a small mean free path for thinner shocks and high Reynolds number studies. In its simplest formulation the relaxation operator becomes implicit by simply setting $g_l^{(+)}$ to $g_l^{(m+1)}$ in Eq. (8). One extracts

$$g_l^{(m+1)} = \frac{g_l^{(*)} + (\nu\,\Delta t)\, g_l^{\mathrm{eq}(*)}}{(1+\nu\,\Delta t)} \xrightarrow[\nu\,\Delta t \gg 1]{} g_l^{\mathrm{eq}(*)} \tag{9}$$

This drives the weights to the equilibrium distribution for large collision rates. A similar expression produces $h_l^{(m+1)}$. Huang *et al.*[13] have streamed

a related equilibrium distribution. A limitation here is that the cycle goes through: (i) streaming, (ii) computation of the moments for $g_l^{eq(*)}$, and then (iii) relaxation yielding $g_l^{(m+1)}$. If the streaming is physically excessive before relaxation, there exists no corrective mechanism. That is, if the local collision rate is high, such that the particles carrying the weights would be converted to a Maxwellian after crossing only a small fraction of a cell width, this is ignored and the particles travel all the way to the next cell center prior to relaxation. A more accurate model would produce a Maxwellian after that first fractional cell width, and then correct the distribution again and again, as the distribution of particles passed each mean free path. Such excess streaming has been ameliorated to some degree by implicitly coupling the streaming and collisional relaxation updates,[32] i.e.,

$$g_l^{(m+1)}(x) = g_l^{(m)}(x - u_l\,\Delta t) - \nu\,\Delta t\{(\theta g_l^{(m+1)}(x) + (1-\theta)\,g_l^{(m)}(x - u_l\,\Delta t)) - (\theta g_l^{eq(*)}(x) + (1-\theta)\,g_l^{eq(m)}(x - u_l\,\Delta t))\} \tag{10}$$

with a similar equation for $h_l^{(m+1)}$. The parameter θ can be set to 0.5 for time centering, and to 1.0 for maximal stability. Equation (10) is a solution to Eq. (3a) along the characteristics of Eq. (7). The implicit relaxation of the weights occurs as a particle streams from the old position $x_l - u_l\,\Delta t$ to the new $x_l = x_i$. *The weights at the end of the particle trajectory are identical to the weights at corresponding nodes, since all the particles move between nodes.* The $\nu\,\Delta t$ terms drive the time-averaged distribution toward the time-averaged Maxwellian. The solution is found iteratively and locally at each node: (1) A guess for $g_l^{eq(*)} = g_i^{eq(*)}$ is made; e.g., we start with the equilibrium Maxwellian following pure streaming. (2) Equation (10) is then solved for the resultant $g_i^{(m+1)} = g_l^{(m+1)}$ at each node. (3) Similarly, $h_i^{(m+1)}$ is obtained. (4) Finally, new moments, n, nU, and na_0^2 are determined from (5), and used to get an improved values for $g_i^{eq(*)}$ and $h_i^{eq(*)} = h_l^{eq(*)}$. Typically, after 3 iterations this process appears to give good convergence. As with traditional particle-in-cell codes, for $\theta = 0.5$ the average force (particle collisions) operates at the average particle positions on the average weights, rendering, we believe, second order accuracy in space and time, although structures (e.g., the contact surface) remain broad due to the large stencil for the macro-cells. This view warrants further study, however. Others have proposed more complex implicit[33] LBM schemes, requiring the solution of elliptic equations avoided here.

Implicit relaxation adds a new degree of control, missing in conventional LBM. Normally, the non-centered transport is mildly dissipative, and the explicit relaxation operation, which is related to an unexpanded Eq. (8) with $(+) = (*)$, could lead to instability or net exponential growth

for $v\,\Delta t > 2$ (i.e., $\tau < \Delta t/2$). Here, the implicit collisions are conservative when centered and otherwise dissipative, assuring stability with $v\,\Delta t \gg 1$.

3. SHOCK TUBE APPLICATION

The success of this approach in 1D is demonstrated with the pictured results of Figs. 2 and 3 for an 8:1 initial density ratio shock tube, and a 10:1 initial pressure jump [initial thermal speed $a_0(x=0)=1$], particle speeds $u_i = +5, +4, +3, \ldots$ to -5, and an initially motionless perfect gas ($\gamma = 5/3$), with $\Delta t = 0.2$, $\Delta x = 0.2$, and with $v\,\Delta t = 100$, implicit streaming and relaxation Eq. (10) with $\theta = 0.55$ time-centering. This is the classical Sod test problem[34] with both a density jump and a temperature step (of 1.25:1). Here Δx is arbitrary, and $\Delta t = \Delta x/a_0$. The moments at $t = 20$ compare well with the exact solution. The resultant shock Mach number is 2.13.

Our full set of results is for 500 cells. Mirror boundary conditions were applied, so that at $x = 0$, for example, a particle on passing through the boundary has its speed and position changed as: $u_l \to -u_l$, and $x_l \to -x_l$. Here, the shock transition takes about 11 computational cells, or one macro-cell. No density overshoots appear in the vicinity of the shock. The calculated contact "surface" is 3 macro-cells wide. Using the simpler Eq. (9) for relaxation the shock is twice as wide. With either relaxation model the results are unchanged for $v\,\Delta t \geqslant 10$. With Eq. (10) the shock is 1.5 times thicker, if $\theta = 1.0$; instability is evident for $\theta < 0.5$. If the time step is reduced by ½ to $\Delta t = 0.1$ with the older area-weighting of density and

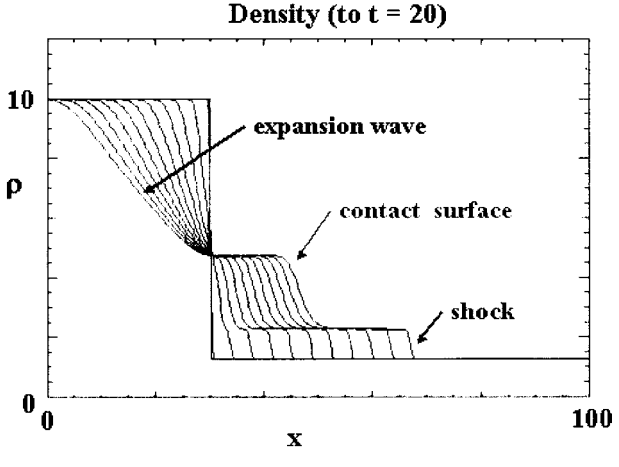

Fig. 2. The evolving density profile up to $t = 20$.

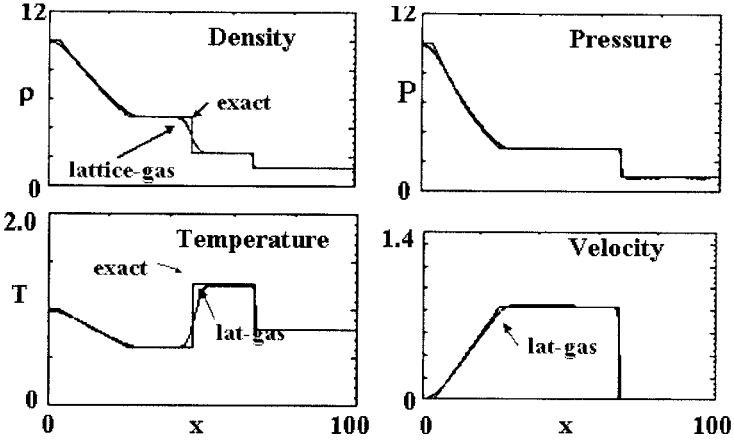

Fig. 3. Normalized density, temperature $T = a_0^2/a_0^2(t = 0, x = 0)$, pressure and velocity as compared to the exact solution to the classical Sod problem, $P_l/P_r = 10$, $\rho_l/\rho_r = 8$, $T_l/T_r = 1.25$.

transverse energy to the mesh, the shock broadens noticeably, as originally in refs. 23 and 24. When, as well, the velocity range was reduce to ± 3.5, the post-shock density profile was erroneously upward slanting toward the shock, since resolution was missing at speeds needed to properly register the shocked temperature rise. This points to a need for higher speed beams in our CLBM, when higher Mach numbers are anticipated.

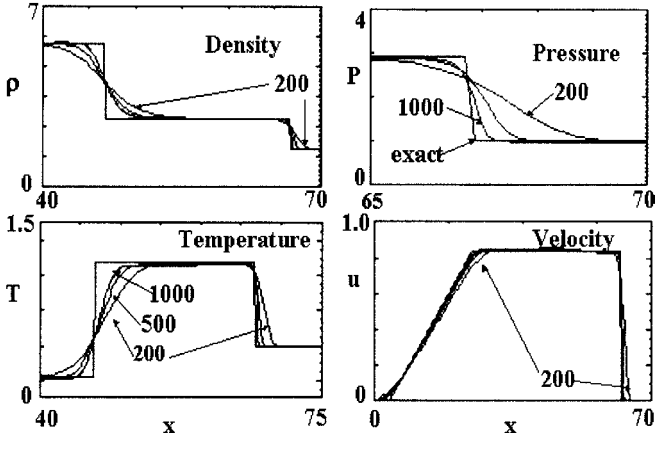

Fig. 4. Convergence test showing the CLBM solution converging toward the exact solution as the number of cells in the test area is changed from 200 to 500, and then to1000.

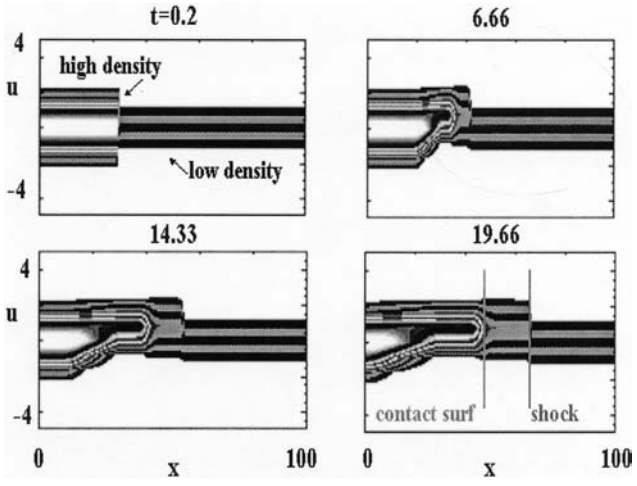

Fig. 5. The phase space constructed from the density weights g_i shows the sub-structure of the evolving shock and contact surfaces.

Figure 3 compares our CLBM results with the exact solution, as determined from software available with ref. 9. The largest discrepancies are at the contact surface. Compared to the same classical Sod shock studied by Prendergast and Xu,[14] which used only 200 cells, our contact surface appears wider. This is likely due to the broad spatial stencil of our CLBM. Figure 4 shows that our results converge toward the exact solution as the number of cells in the test area is increase from 200 to 500, plus results for a further cell increase to 1000. In Fig. 5 the phase space accumulation (for 500 cells) of density weights shows the underlying structure of the evolving shock, contact surface, and expansion at times approaching $t = 20$.

4. OBSERVATIONS

Advantages of our new CLBM are simplicity, ease of implementation—even with implicit relaxation, and accuracy with minimal overshoots and diffusion as demonstrated in our shock tube tests. The new scheme relates to other and older DVM kinetic methods, but uses a much smaller number of speeds, and concentrates on the Eulerian limit. It extends LBM by avoiding the low mean velocity expansion of f^{eq} that leads to a breakdown of the standard method beyond moderate Mach numbers, e.g., $M > 0.35$, as reported by Vahala *et al.*[18] It avoids the velocity overshoots of thermal models with extended velocities, as seen by Guangwu *et al.*,[21] and the ambiguities in the choice of additional moment equations

encountered in closing such models. It avoids unphysical dissipation from limitation (near shocks) required for alternate gas kinetic BGK models,[14–16] by using a strict space-velocity lattice as in conventional LBM, but with an extended stencil of cells. Unlike other newer methods, e.g., ref. 19, it should provide stable access to low Reynolds numbers (for $\nu\,\Delta t \gg 1$, i.e., $\tau/\Delta t \ll 1$) via implicit collisional relaxation. Our CLBM approach yields useful insight into the underpinnings of the Lattice-Boltzmann Method, and offers the serious possibilities for productive future extensions.

It is instructive to compare the well-regarded Gas-Kinetic approach of Prendergast and Xu to our CLBM technique. These authors show in ref. 14, Eq. (2.15) that the formal solution to our BGK equation (1) over a time step $\Delta t = t - t_0$ for a fixed collision rate $\nu = 1/\tau$ is given by the sum of the streamed initial distribution times an exponential decay factor $e^{-t/\tau}$, plus the time integral from $t' = t_0 = 0$ to $t' = \Delta t$ of the local Maxwellian equilibrium distribution $f^{\text{eq}}(t')$ times the exponential kernal $e^{-(t-t')/\tau}$. They evaluate this Maxwellian approximately as a linear extrapolation in x and t of its values from the cell boundaries. Conservation of moments is employed to determine the extrapolation coefficients in x and t. This leads to moment fluxes, which must be limited to determine smooth and stable hydrodynamics.

Alternatively, our CLBM approach time-centers a spatially cell-centered f^{eq} for our choice of θ, moves it outside the integral sign, and time integrates just the remaining exponential kernal. With the subsequent approximation that $e^{-t/\tau} \approx 1/(1+\Delta t/\tau) = 1/(1+\nu\,\Delta t)$, we obtain Eq. (8). We then implicitly determine f^{eq} at the cell centers by local iteration. This appears to be a simpler procedure, yielding, for example, good agreement with the exact solution to our shock problem.

Two obvious options exist for higher dimensions. The most accurate approach would be to square the number of velocities for 2D, and move the particles to particle centers in the square surrounding an emitting cell, as done in conventional LBM, but with the extra velocities. This minimizes mesh related errors, say along the 45° directions. In 2D this would require $11^2 = 121$ speeds. While such a large speed count is unusual, given the embarrassingly parallel nature of CLBM, this direct approach could be used with newly developing DOE-ASCI computing resources (at least for 2D), allowing for efficient domain decomposition[35] and parallel scaling. The details of such an implementation must await further study. A simpler approach, as suggested by both Prendergast and Xu[14] and by ref. 22, could be to *operator-split* the hydrodynamics into the maximum number of directions, i.e., three successive one-dimensional problems for 3D, and then updates weights sequentially in each of these directions, alternating the directions in successive time steps. No more than the one-dimensional total

(e.g., 11) of velocity beams—repeatedly re-weighted and generating new intermediate moments—might suffice for this approach. While this would sacrifice some multi-dimensional advantages of LBM, it would still avoid the need for Riemann solutions, and the introduction of numerical diffusion from flux limitation.

Our focus here has been Eulerian flow. Generally, the effective mean free path λ equals a_0/ν. For $\nu \Delta t \geqslant 1$ our model approximates the viscous Navier–Stokes equations with the usual Krook equation limitations,[4, 16, 22] e.g., that the Prandtl number is unity, with additional deviations that arise from the limited number of velocities employed. This still needs quantitatively evaluation. The Prandtl number can be adjusted with modifications in the equilibrium distribution,[36] f^{eq}. Similarly, generalizations[37] of the classical LBM can allow for realistic Prandtl numbers in incompressible flows. A rough mock-up of free-molecular flow would be obtained for $\nu \Delta t \ll 1$, with accuracy that can be augmented by the increasing number of streaming velocities employed in the modeling.

The new method requires a large spatial stencil required for the particles to move strictly between cell centers. An alternate scheme, transporting the fastest particles to just the next cell center, would give the "tightest" description. The slower particles would then only partially cross a cell, making contributions to only the nearest cell neighbors. However, without recourse to TVD-type corrections, which drove us from traditional Eulerian modeling in the first place, such tight stencils appear to manifest excessive interpolative diffusion, as discussed with Fig. 1. An alternate view is that the 11 cells comprising a macro-cell are providing a natural diffusion-minimized sub-structure for the coupled transport and relaxation in LBM.

For studies of the turbulent mix of multiple materials a logical direction for extension of the CLBM is to introduce Krook equations for each component, and couple them through extended relaxation operators, as explored in refs. 38 and 16. The transverse energy component can be generalized to allow for varied EOS choices.[39, 40] Finally, adaptive mesh refinement can be accomplished, as suggested by refs. 41 and 42, particularly near shocks and contact surfaces to reduce overall computational demands.

5. CONCLUSION

We have shown that the Lattice-Boltzmann Method extends to compressible problems via a simple scheme, using a relatively small number of velocities on a large stencil. Particles jump over the neighboring cells on a velocity-space lattice that avoids interpolative diffusion. Retention of an unexpanded Maxwellian simplifies the calculations immensely. Implicit

collisional relaxation affords stability, and access to high collision rates, while preserving an option for straightforward parallelism. Our shock tube application demonstrates no overshoots, and a close approximation the exact solution. The method is simpler than gas-kinetic schemes, works at higher Mach numbers than thermal LBM models, and avoids the ambiguities introduced with an expanded Maxwellian equilibrium requiring many moments. Still, other methods may be preferred. Our aim has been principally to provide new insight, a discussion of specific advantages and limitations of the new CLBM method, and suggestions for possible extensions.

ACKNOWLEDGMENTS

The author is grateful for enlightening and encouraging discussions with Tim Clark, Xiaoyi He, Shiyi Chen, and Gary Doolen at Los Alamos. This work was performed under the auspices of the U.S.D.O.E.

REFERENCES

1. U. Frisch, B. Hasslacher, and Y. Pomeau, Lattice gas automata for the Navier–Stokes equation, *Phys. Rev. Lett.* **56**:1505 (1986).
2. G. McNamara and G. Zanetti, Use of the Boltzmann equation to simulate lattice-gas automaton, *Phys. Rev. Lett.* **61**:2332 (1998).
3. S. Chen, H. D. Chen, D. Martinez, and W. Matthaeus, Lattice Boltzmann model for simulation of magnetohydrodynamics, *Phys. Rev. Lett.* **67**:3776 (1991); H. Chen, S. Chen, and S. Mattaeus, *Phys. Rev. A* **45**:R5339 (1992).
4. P. L. Bhatnagar, E. P. Gross, and M. Krook, A model for collision processes in gases, I. Small amplitude processes in charged and neutral one-component systems, *Phys. Rev.* **94**:511 (1954).
5. S. Chen and G. Doolen, Lattice Boltzmann method for fluid flows, *Annu. Rev. Fluid Mech.* **30**:329 (1998).
6. X. He, R. Zhang, S. Chen, and G. Doolen, On the three-dimensional Rayleigh–Taylor instability, *Phys. Fluids* **11**:1143 (1999).
7. R. J. Mason, A compressible Lattice-Boltzmann model, *Bull. Am. Phys. Soc.* **45**:168 (2000).
8. J. P. Boris and D. Book, Flux-corrected transport I. SHASTA, A fluid transport algorithm that works, *J. Comput. Phys.* **11**:38 (1973).
9. E. F. Toro, *Riemann Solvers and Numerical Methods for Fluid Dynamics*, 2nd ed. (Springer-Verlag, Berlin, 1999).
10. F. Grasso and C. Meola, Euler and Navier–Stokes equations for compressible flows: Finite-volume methods, *Handbook of Computational Fluid Mechanics*, R. Peyret, ed. (Academic Press, San Diego, 1996), p. 159.
11. F. J. Alexander, H. Chen, S. Chen, and G. D. Doolen, Lattice Boltzmann model for compressible fluids, *Phys. Rev. A* **46**:1967 (1992).
12. B. T. Nadiga, An Euler solver based on locally adaptive discrete velocities, *J. Statist. Phys.* **81**:129 (1995).

13. J. Huang, F. Xu, M. Vallieres, D. H. Feng, Y.-H. Qian, B. Fryxell, and M. R. Strayer, A thermal LBGK model for large density and temperature differences, *Internat. J. Modern Phys. C* **8**:827 (1997).
14. K. H. Prendergast and K. Xu, Numerical hydrodynamics from gas-kinetic theory, *J. Comput. Phys.* **109**:53 (1993).
15. C. Kim, K. Xu, L. Martinelli, and A. Jameson, Analysis and implementation of the gas-kinetic BGK scheme for computational gas dynamics, *Internat. J. Numer. Methods Fluids* **25**:21 (1997).
16. A. D. Kotelnikov and D. C. Montgomery, A kinetic Method for computing inhomogeneous fluid behavior, *J. Comput. Phys.* **134**:364 (1997).
17. A. Renda, G. Bella, S. Succi, and I. V. Karlin, Thermohydrodynamic lattice BGK schemes with non-perturbative equilibria, *Europhys. Lett.* **41**:279 (1998).
18. G. Vahala, P. Pavlo, L. Vahala, and N. S. Martys, Thermal lattice-Boltzmann models (TLBM) for compressible flows, *Internat. J. Modern Phys. C* **9**:1247 (1998).
19. C. Sun, Lattice-Boltzmann model for high speed flows, *Phys. Rev. E* **58**:7283 (1998).
20. M. De Cicco, S. Succi, and G. Bella, Nonlinear stability of compressible thermal lattice BGK models, *SIAM J. Sci. Comput.* **21**:366 (1999).
21. Y. Guangwu, C. Yaosong, and H. Shouxin, Simple lattice Boltzmann model for simulating flows with shock wave, *Phys. Rev. E* **59**:454 (1999).
22. Y. Yang and J. C. Huang, Rarefied flow computations using nonlinear model Boltzmann equations, *J. Comput. Phys.* **120**:323 (1995).
23. R. J. Mason and C. K. Chu, A particle-in-cell method for model kinetic equations, *Rarefied Gas Dynamics*, Vol. II, Seventh Symposium, D. Dini and C. Cercignani, eds. (Editrice, Tecnico Scientifica, Pisa, Italy, 1971), p. 889.
24. C. K. Chu, W. P. Gula, and R. J. Mason, A modified particle-in-cell Method for Collisional Plasmas, *Proceedings of the Fourth Conference on Numerical Simulation of Plasmas*, J. P. Boris and R. A. Shanny, eds. (Naval Research Laboratory, Washington, D.C., 1970), p. 30.
25. W. P. Gula and C. K. Chu, Effect of Krook model collisions on the two-stream instability, *Phys. Fluids* **16**:1135 (1973).
26. C. K. Chu, Kinetic-theoretic description of shock wave formation II, *Phys. Fluids* **8**:1450 (1965).
27. C. K. Birdsall and A. B. Langdon, *Plasma Physics via Computer Simulation* (McGraw Hill, New York, 1985).
28. R. J. Mason, Weak shock generation according to the energy-conserving Bhatnagar–Gross–Krook kinetic equation, *Phys. Fluids* **13**:1467 (1970).
29. L. Mieussens, Discrete-Velocity Models and numerical schemes for the Boltzmann-BGK equation in plane and axisymmetric geometries, *J. Comput. Phys.* **162**:429–466 (2000).
30. L.-S. Luo, Some recent results on discrete velocity models and ramifications for lattice Boltzmann equation, *Comput. Phys. Comm.* **129**:63–74 (2000).
31. X. He, S. Chen, and G. Doolen, A novel thermal model for the lattice Boltzmann method in incompressible limit, *J. Comput. Phys.* **146**:282–300 (1997).
32. K. Sankaranarayanan, X. Shan, I. G. Kevrekidis, and S. Sundaresan, Analysis of drag and virtual mass forces in bubbly suspensions using an implicit formulation of the lattice Boltzmann method, to be published.
33. J. Tölke, M. Krafczyk, M. Schulz, E. Rank, and R. Berrios, Implicit discretization and nonuniform mesh refinement approaches for FD discretizations of LBGK models, *Internat. J. Modern Phys. C* **9**:1143 (1998).
34. G. A. Sod, A Numerical Study of Converging Cylindrical Shocks, *J. Fluid Mech.* **83**:78–794 (1977).

35. N. Satofuka and T. Nishioka, Parallelization of lattice Boltzmann method for incompressible flow computations, *Comput. Mech.* **23**:164 (1999).
36. H. Holway, Kinetic theory of shocks using an ellipsoidal distribution function, *Rarefied Gas Dynamics*, Fourth Symposium, J. H. de Leeuw, ed. (Academic Press, New York, 1965), p. 193.
37. P. Lallemand and Li-Shi Luo, Theory of the lattice Boltzmann method: Dispersion, dissipation, isotropy, Galilean invariance, and stability, *Phys. Rev. E* **61**:6546 (2000).
38. T. F. Morse, Kinetic model equations for a gas mixture, *Phys. Fluids* **7**:2012 (1964).
39. H. Struchtrup, The BGK model for an ideal gas with an internal degree of freedom, *Transport Theory Statist. Phys.* **28**:369 (1999).
40. P. Andries, P. Le Tallec, J-P. Perlat, and B. Perthame, The Gaussian-BGK model of Boltzmann equation with small Prandtl number, *Eur. J. Mech. B Fluids* **19**:813 (2000).
41. D. Kandhai, W. Soll, S. Chen, A. Hoekstra, and P. Sloot, Finite-difference lattice-BGK methods on nested grids, *Comput. Phys. Comm.* **129**:100 (2000).
42. D. Yu, R. Mei, and Wei Shyy, A Multi-block Lattice Boltzmann Method for fluid flows, Aeronautics and Astronautics, to be published.